

## Modeling of Two-Dimensional Electron Gas Sheet in FDTD Method

Žilvinas Kancleris, Gediminas Šlekas, and Algirdas Matulis

**Abstract**—The technique for implementation of two-dimensional electron gas (2DEG) sheet in a finite-difference time-domain (FDTD) scheme is proposed. The modified electromagnetic field update equations are derived differing from the standard Yee equations by the tangential components of the electric field in the 2DEG plane. The reliability of the proposed technique is checked applying it to the simple problem—the electromagnetic wave reflection dependence on the surface conductivity of 2DEG sheet over-covering wholly cross-section of the rectangular waveguide, and comparing the obtained results with the available analytical solution.

**Index Terms**—Finite-difference time-domain (FDTD) method, surface conductivity, two-dimensional electron gas (2DEG).

### I. INTRODUCTION

Rapid progress of high-frequency electronics stimulates wide application of structures with 2DEG as their active components. Microwave detectors [1], [2], charge-coupled devices [3], active surface acoustic wave filters [4] are only a small part of the growing amount of examples where 2DEG are used. The typical example of the 2DEG is a quantum well in which the quantization freezes the perpendicular motion of electrons and converts them into two-dimensional system with large mobility that appears due to reduction of electron collision rate with impurities.

It is worth mentioning that there are several methods proposed for the approximate numerical simulation of electrically thin material sheets in the FDTD method [5]. These methods handle with two parameters—bulk conductivity and thickness of the layer—characterizing the sheet, what often is not convenient due to the problems of measuring these values. Meanwhile in the classical electrodynamics there is a standard method of dealing such ultra-thin structures [6], namely, by introducing surface charges and currents. The purpose of this communication is to illustrate how such surface currents can be included into numerical FDTD modeling. The advantage of the proposed technique is that in this case the thin sheet is characterized by a single parameter the surface conductivity  $\sigma_s$  that is quite adequate for description of the above mentioned 2DEG.

### II. FDTD FIELD UPDATE EQUATIONS FOR 2DEG

Let us assume that we are modeling the behavior of the electromagnetic field in a homogeneous space characterized by permeability  $\mu$  and permittivity  $\varepsilon$  with a single 2DEG sheet included in the  $xy$  plane at the point  $z = z_k$ . Considering surface currents in the sheet we have to modify a single Maxwell equation, namely, the Ampère's law rewriting it as follows:

$$\frac{\partial \mathbf{E}}{\partial t} = \frac{1}{\varepsilon} \{ \text{rot} \mathbf{H} - \mathbf{E}_{\parallel} \sigma_s \delta(z - z_k) \} \quad (1)$$

Manuscript received April 24, 2012; revised September 05, 2012; accepted October 11, 2012. Date of publication October 19, 2012; date of current version January 30, 2013. This work was supported in part by a grant (No. MIP-092/2011) from the Research Council of Lithuania.

Ž. Kancleris and G. Šlekas are with the Department of Physical Technologies, Semiconductor Physics Institute of Center for Physical Sciences and Technology, LT-01108 Vilnius, Lithuania (e-mail: kancleris@pfi.lt; slekas@pfi.lt).

A. Matulis is with the Department of Fundamental Research, Semiconductor Physics Institute of Center for Physical Sciences and Technology, LT-01108 Vilnius, Lithuania (e-mail: amatulis@takas.lt).

Color versions of one or more of the figures in this communication are available online at <http://ieeexplore.ieee.org>.

Digital Object Identifier 10.1109/TAP.2012.2225819

here  $\mathbf{E}$  is the strength of electric field,  $\mathbf{E}_{\parallel}$ —the electric field component in the sheet plane, and  $\mathbf{H}$  is the strength of magnetic field. The symbol  $\delta(z)$  stands for the Dirac function that is often used when dealing with an infinitely thin and infinitely high spikes in the coefficients of differential equations.

Standard Yee discretization scheme [7] with 2DEG sheet superimposed on it is shown in Fig. 1. It is obvious that outside the shadowed  $\Delta z$  thickness layer the standard Yee discretization scheme can be applied, whereas inside it more sophisticated approach should be used. In fact, (1) should be integrated within the layer eliminating in this way its ambiguity due to Dirac function. To do that we perform the discretization of (1) on coordinates  $x$ ,  $y$  and time  $t$  only, and get the following equation for  $y$  component of the electric field in the plane  $y = (j + 1/2)\Delta y$  suitable for integration within the mentioned above layer:

$$\begin{aligned} & \frac{\varepsilon \left( E_y \Big|_i^{n+1}(z) - E_y \Big|_i^n(z) \right)}{\Delta t} \\ &= \frac{\partial H_x}{\partial z} \Big|_i^{n+1/2}(z) - \frac{H_z \Big|_{i+1/2}^{n+1/2}(z) - H_z \Big|_{i-1/2}^{n+1/2}(z)}{\Delta x} \\ & \quad - \frac{\sigma_s}{2} \left( E_y \Big|_i^{n+1}(z) + E_y \Big|_i^n(z) \right) \delta(z - z_k) \end{aligned} \quad (2)$$

where the superscript  $n$  corresponds to the time  $t$ , the indexes  $i, j$ —to the coordinates, and the symbols of type  $\Delta x$  stand for the discretization steps along the corresponding axes and time. In this and further equations index  $j$  is omitted since it has the same value  $j + 1/2$  in all terms. To proceed further (2) should be integrated along  $z$  axis eliminating  $\delta(z)$  function. As follows from Fig. 1, it should be performed between  $z_{k-1/2}$  and  $z_{k+1/2}$ . Integration of the derivative in (2) leads to the difference of  $H_x$  at the integration limits, whereas the last term of the equation due to  $\delta(z)$  function gives  $E_y$  value at  $z_k$ . Integrating the rest two terms by the simplest rectangle method we get the desirable value of components  $E_y$  and  $H_z$  at  $z = z_k$ . As a result we obtain the difference equation that is matched with Yee scheme:

$$\begin{aligned} & \frac{\varepsilon \Delta z}{\Delta t} \left( E_y \Big|_{i,k}^{n+1} - E_y \Big|_{i,k}^n \right) = \left( H_x \Big|_{i,k+1/2}^{n+1/2} - H_x \Big|_{i,k-1/2}^{n+1/2} \right) \\ & \quad - \frac{\Delta z}{\Delta x} \left( H_z \Big|_{i+1/2,k}^{n+1/2} - H_z \Big|_{i-1/2,k}^{n+1/2} \right) - \frac{\sigma_s}{2} \left( E_y \Big|_{i,k}^{n+1} + E_y \Big|_{i,k}^n \right). \end{aligned} \quad (3)$$

Collected and isolated  $E_y \Big|_{i,k}^{n+1}$  terms on the left hand side of (3) lead to the desired explicit time-stepping relation for  $E_y$

$$\begin{aligned} E_y \Big|_{i,k}^{n+1} &= \left( \frac{1 - \frac{\sigma_s \Delta t}{2\varepsilon \Delta z}}{1 + \frac{\sigma_s \Delta t}{2\varepsilon \Delta z}} \right) E_y \Big|_{i,k}^n + \frac{\frac{\Delta t}{\varepsilon}}{1 + \frac{\sigma_s \Delta t}{2\varepsilon \Delta z}} \\ & \quad \times \left[ \frac{H_x \Big|_{i,k+1/2}^{n+1/2} - H_x \Big|_{i,k-1/2}^{n+1/2}}{\Delta z} - \frac{H_z \Big|_{i+1/2,k}^{n+1/2} - H_z \Big|_{i-1/2,k}^{n+1/2}}{\Delta x} \right]. \end{aligned} \quad (4)$$

In the same way the analogous equation for iterating  $E_x$  component is obtained. Compared to the standard expressions for calculation of  $E_x$  and  $E_y$  components in lossy materials [8] the only difference is that bulk conductivity  $\sigma$  in 2DEG case is replaced with  $\sigma_s / \Delta z$ . These

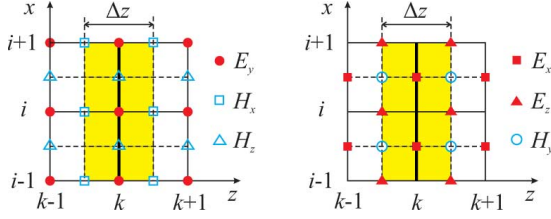


Fig. 1. 2DEG sheet shown by thicker line superimposed on Yee discretization scheme [7]. Numerical integration region is shadowed. Left—components in  $y = (j + 1/2)\Delta y$  plane, right—in  $y = j\Delta y$  plane.

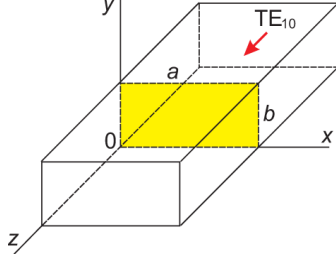


Fig. 2. The layout of the  $TE_{10}$  wave scattering in the rectangular waveguide by the perpendicular 2DEG sheet.

tangential electric field components outside the sheet and all other components of the electromagnetic field has to be calculated by means of the standard update equations [8].

### III. CALCULATION RESULTS AND DISCUSSION

In order to illustrate the efficiency of the proposed method we modeled the propagation of  $TE_{10}$  electromagnetic wave along the rectangular waveguide which is divided into two parts by the 2DEG sheet as it is shown in Fig. 2 by shadowed rectangle at the point  $z = 0$ .

The matter is that due to the simple geometry this problem enables to obtain the analytic solution based on the matching at the interface  $z = 0$  the incident, reflected and transmitted waves with the same  $(x, y)$  dependence, namely, to solve the scattering problem restricting the consideration only by a single mode. We used this analytic result for the estimation of the numerical modeling accuracy. Indeed, due to the infinitesimal thickness of the 2DEG sheet we have to solve the problem in both parts of the empty waveguide outside the above sheet ( $z < 0$  and  $z > 0$ ). These solutions can be expressed via the longitudinal (perpendicular to the 2DEG sheet) field components that satisfies the two-dimensional wave equation which leads to the following dispersion relation:

$$\omega^2 - \omega_c^2 = c^2 k^2 \quad (5)$$

for cycling frequency  $\omega = 2\pi f$ , wave vector  $k$ , and the cutoff frequency

$$\omega_c = 2\pi f_c = \gamma c, \quad \gamma = \frac{\pi}{a} \quad (6)$$

where  $c$  is the velocity of light in free space. Presented here dispersion relation can be found in textbooks on electrodynamics (see, for instance [9]). So, we assumed that before the sheet (in the region  $z < 0$ ) there are the incident and reflected  $TE_{10}$  modes with transverse electromagnetic field components

$$E_y = E_0 e^{-i\omega t} \left\{ e^{ikz} + R e^{-ikz} \right\} \sin(\gamma x) \quad (7a)$$

$$H_x = -\frac{ck}{\omega Z_0} E_0 e^{-i\omega t} \left\{ e^{ikz} - R e^{-ikz} \right\} \sin(\gamma x) \quad (7b)$$

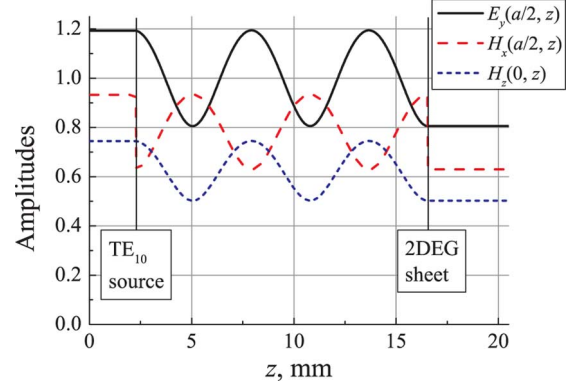


Fig. 3. Distributions of the electromagnetic field components in the center of the rectangular waveguide with 2DEG sheet. Calculation parameters:  $a = 7.2$  mm,  $f = 33.4$  GHz,  $\sigma_s = 10^{-3}$  S,  $\Delta x = 0.03$  mm,  $\Delta z = 0.03$  mm.

where  $Z_0$  is the impedance of free space. Behind the sheet (in the region  $z > 0$ ) there is a transmitted wave with the components

$$E_y = E_0 e^{-i\omega t} T e^{ikz} \sin(\gamma x) \quad (8a)$$

$$H_x = -\frac{ck}{\omega Z_0} E_0 e^{-i\omega t} T e^{ikz} \sin(\gamma x). \quad (8b)$$

At the interface ( $z = 0$ ) the electric field components are continuous (because we neglect the surface charges on the conductive sheet), and the longitudinal magnetic field component is continuous as well. Due to Dirac function in (1) the transverse magnetic field components suffer the breaks proportional to the surface current what in our case can be presented as

$$\Delta H_x = \sigma_s E_y. \quad (9)$$

Satisfying the above boundary conditions for  $E_y$  and  $H_x$  components on the sheet (the boundary condition for the longitudinal  $H_z$  component is satisfied automatically) we obtain the following set of algebraic equation

$$1 + R = T, \quad (10a)$$

$$-\frac{ck}{\omega Z_0} \{T - (1 - R)\} = \sigma_s (1 + R) \quad (10b)$$

which solution gives us the reflection coefficient

$$R = -\frac{\sigma_s Z_0}{\sigma_s Z_0 + 2\sqrt{1 - \left(\frac{f_c}{f}\right)^2}}. \quad (11)$$

Longitudinal distributions of the amplitudes of the electromagnetic field components in the center of the waveguide with 2DEG sheet calculated using FDTD procedure are presented in Fig. 3. All the amplitudes are normalized to the  $E_0$ —the strength of the electric field in the center of the empty waveguide, the magnetic field amplitudes are multiplied by  $Z_0$ , so they have the same units of measurement as the electric field.

Making use of the electric field distribution in the region between the wave source and 2DEG sheet (vertical solid lines in Fig. 3) we defined the reflection coefficient  $R$ .

The dependencies of the absolute value of the reflection coefficient  $R$  on the surface conductance  $\sigma_s$  are shown in Fig. 4 for two different frequencies and  $\Delta z$  values. As one can see from the figure, values of the reflection coefficient obtained numerically (Fig. 4 dots) fits well the analytical solution (11) (Fig. 4 solid line). It is seen that in the considered step size range the result is independent of  $\Delta z$  though it appears in the approximation of the 2DEG sheet conductivity in (4). The calculation error of  $R$  values are of the same order as the accuracy limit

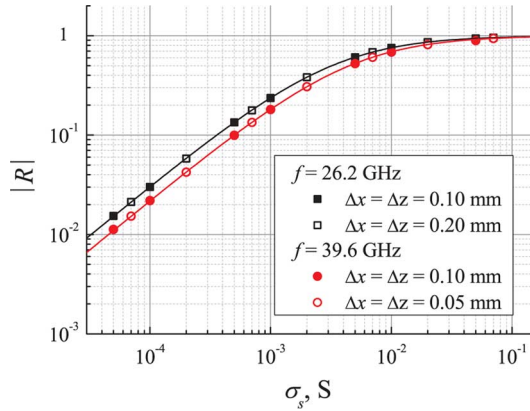


Fig. 4. Dependence of the absolute value of the reflection coefficient on 2DEG sheet's surface conductivity. Points correspond to the FDTD modeling, solid lines show the analytical solution (11).  $a = 7.2$  mm.

due to not perfect absorbing boundary conditions. It should be pointed out that the electric field near the 2DEG sheet in this particular case depends only on  $R$ , so a high precision of  $R$  automatically leads to the precise values of the electromagnetic field components in the whole model. Therefore results presented in Fig. 4 validates the reliability of proposed modification to the FDTD update equations in 2DEG area.

#### IV. CONCLUSION

The technique was developed for modeling two-dimensional sheets, the properties of which are characterized by surface conductivity. The 2DEG layer was included in FDTD scheme by simply modifying the update equations of the nodes of tangential electric field components located in the plane of the sheet. Results of numerical calculation of reflection coefficient from the 2DEG layer filling rectangular waveguide's cross-section show a good agreement with analytically obtained solution.

#### REFERENCES

- [1] D. Seliuta, E. Širmulis, V. Tamošiūnas, S. Balakauskas, S. Ašmontas, A. Suziedelis, J. Gradauskas, G. Valušis, A. Lisauskas, H. G. Roskos, and K. Köhler, "Detection of terahertz n sub-terahertz radiation by asymmetrically-shaped 2DEG layers," *Electron. Lett.*, vol. 40, no. 10, pp. 631–632, 2004.
- [2] D. Seliuta, I. Kašalynas, V. Tamošiūnas, S. Balakauskas, Z. Martunas, S. Ašmontas, G. Valušis, A. Lisauskas, H. G. Roskos, and K. Köhler, "Silicon lens-coupled bow-tie InGaAs-based broadband terahertz sensor operating at room temperature," *Electron. Lett.*, vol. 42, no. 10, pp. 825–827, 2006.
- [3] E. R. Fossum, J.-I. Song, and D. V. Rossi, "Two-dimensional electron gas charge-coupled devices (2DEG-CCD's)," *IEEE Trans. Electron Dev.*, vol. 38, no. 5, pp. 1182–1192, 1991.
- [4] F. Calle, J. Grajal, and J. Pedrós, "Active saw devices on 2DEG heterostructures," *Electron. Lett.*, vol. 40, no. 21, pp. 1384–1386, 2004.
- [5] J. G. Maloney and G. S. Smith, "A comparison of methods for modeling electrically thin dielectric and conducting sheets in the finite-difference time-domain (FDTD) method," *IEEE Trans. Antennas Propag.*, vol. 41, no. 5, pp. 690–694, 1993.
- [6] J. Jin, *Theory and Computation of Electromagnetic Fields*. Hoboken, NJ: Wiley, 2010, ch. 5.4.
- [7] K. S. Yee, "Numerical solution of initial boundary value problems involving Maxwell's equations in isotropic media," *IEEE Trans. Antennas Propag.*, vol. 14, no. 3, pp. 302–307, 1966.
- [8] A. Taflov and S. C. Hagness, *Computational Electrodynamics: The Finite-Difference Time-Domain Method*. Norwood, MA: Artech House, 2000.
- [9] J. D. Jackson, *Classical Electrodynamics*. New York: Wiley, 1998, ch. 8.4.

## FDTD Dispersive Modeling of Human Tissues Based on Quadratic Complex Rational Function

Sang-Gyu Ha, Jaehoon Cho, Jaehoon Choi, Hyeongdong Kim, and Kyung-Young Jung

**Abstract**—We propose a dispersive finite-difference time domain (FDTD) suitable for the electromagnetic analysis of human tissues. The dispersion relation of biological tissues is characterized by a quadratic complex rational function (QCRF) that leads to an accurate FDTD algorithm in 400 MHz–3 GHz. QCRF coefficients are extracted by applying the complex-curve fitting technique, without initial guess. Numerical examples are used to illustrate the computational accuracy and stability of QCRF-based FDTD.

**Index Terms**—Biological tissues, curve fitting, dispersive media, FDTD methods.

#### I. INTRODUCTION

The finite-difference time domain (FDTD) method [1], [2] has been widely used to analyze complex media such as metalodielectric nanostructures [3], magnetic dispersive media [4], and random inhomogeneous media [5] due to its accuracy, robustness, and easy (matrix-free) implementation. Recently, researches on the interaction of electromagnetic (EM) waves and biological bodies have received increasing attention due to their promising applications in medical sensors and personal diagnostic information [6]–[8]. These applications include medical implant communication service (MICS), wireless medical telemetry service (WMTS), and medical body area network (BAN) and also industrial, scientific and medical (ISM) band is used for medical applications.

Frequency dependent permittivity and conductivity values for human tissues have been compiled by Gabriel [9], where they have been fitted by the 4-pole Cole-Cole equation [10]. This dispersion model characterizes accurately many types of biological tissues over a very wide frequency band. Due to the fractional order differentiator, however, its FDTD implementation is extremely complicated, leading to overwhelming computational burdens. Alternatively, Debye dispersion models can be used, including one-pole Debye model [11], extended one-pole Debye model [12], two-pole Debye model [13], and extended two-pole Debye model [14] (here the conductivity term is included in extended Debye models). For example, the one-pole Debye model is suitable for the dispersion modeling of human body in ultrawideband (UWB) band (3–11 GHz) [11]. However, this model cannot be used for the frequency band where the variation of relative permittivity of human tissues becomes large (e.g., below 1 GHz). Therefore, more complicated Debye models should be used in the frequency band below 1 GHz. However, for Debye dispersion models, a complicated optimization technique (based on Newton's method and least square fitting) should be used to find coefficients of Debye dispersion models. In this case, the initial values are very critical to find accurate coefficients and thus these dispersion models may lead to inaccurate results, as mentioned in [14].

Manuscript received May 16, 2012; revised August 03, 2012; accepted September 19, 2012. Date of publication October 09, 2012; date of current version January 30, 2013. This work was supported by the KCC (Korea Communications Commission), Korea, under the R&D program supervised by the KCA (Korea Communications Agency) (KCA-2011-11911-01109).

The authors are with the Department of Electronics Computer Engineering, Hanyang University, Seoul 133-971, Korea (e-mail: kyung3@hanyang.ac.kr).

Color versions of one or more of the figures in this communication are available online at <http://ieeexplore.ieee.org>.

Digital Object Identifier 10.1109/TAP.2012.2223448